Available online at www.sciencedirect.com

SciVerse ScienceDirect

journal homepage: www.elsevier.com/locate/he

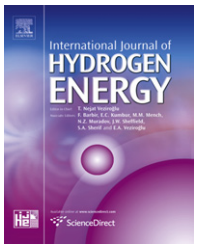

Mechano-chemical synthesis of manganese borohydride ($Mn(BH_4)_2$) and inverse cubic spinel (Li_2MnCl_4) in the ($nLiBH_4 + MnCl_2$) ($n = 1, 2, 3, 5, 9$ and 23) mixtures and their dehydrogenation behavior

R.A. Varin [a,*], L. Zbroniec [a], M. Polanski [b], Y. Filinchuk [c], R. Černý [d]

[a] Department of Mechanical and Mechatronics Engineering, University of Waterloo, 200 University Ave. W, Waterloo, Ontario N2L 3G1, Canada

[b] Faculty of Advanced Technology and Chemistry, Military University of Technology, 2 Kaliski Str., 00-908 Warsaw, Poland

[c] Institute of Condensed Matter and Nanosciences, Université Catholique de Louvain, B-1348 Louvain-la-Neuve, Belgium

[d] Laboratoire de Cristallographie, 24, quai Ernest-Ansermet, CH-1211 Geneva 4, Switzerland

ARTICLE INFO

Article history:
Received 4 June 2012
Received in revised form
31 July 2012
Accepted 2 August 2012
Available online 30 August 2012

Keywords:
Hydrogen storage materials
Ball milling
Manganese borohydride
Nano nickel additives
X-ray diffraction

ABSTRACT

Manganese borohydride ($Mn(BH_4)_2$) was successfully synthesized by a mechano-chemical activation synthesis (MCAS) from lithium borohydride ($LiBH_4$) and manganese chloride ($MnCl_2$) by applying high energy ball milling for 30 min. For the first time a wide range of molar ratios $n = 1, 2, 3, 5, 9$ and 23 in the ($nLiBH_4 + MnCl_2$) mixture was investigated. During ball milling for 30 min the mixtures release only a very small quantity of H_2 that increases with the molar ratio n but does not exceed ~0.2 wt.% for $n = 23$. However, longer milling duration leads to more H_2 released. For the equimolar ratio $n = 1$ the principal phases synthesized are Li_2MnCl_4, an inverse cubic spinel phase, and the $Mn(BH_4)_2$ borohydride. For $n = 2$ a LiCl salt is formed which coexists with $Mn(BH_4)_2$. With the n increasing from 3 to 23 $LiBH_4$ is not completely reacted and its increasing amount is retained in the microstructure coexisting with LiCl and $Mn(BH_4)_2$. Gas mass spectrometry during Temperature Programmed Desorption (TPD) up to 450 °C shows the release of hydrogen as a principal gas with a maximum intensity around 130–150 °C accompanied by a miniscule quantity of borane B_2H_6. The intensity of the B_2H_6 peak is 200–600 times smaller than the intensity of the corresponding H_2 peak. In situ heating experiments using a continuous monitoring during heating show no evidence of melting of $Mn(BH_4)_2$ up to about 270–280 °C. At 100 °C under 1 bar H_2 pressure the ball milled $n = 2$ and 3 mixtures are capable of desorbing quite rapidly ~4 wt.% H_2 which is a very large amount of H_2 considering that the mixture also contains 2 mol of LiCl salt. The H_2 quantities experimentally desorbed at 100 and 200 °C do not exceed the maximum theoretical quantities of H_2 expected to be desorbed from $Mn(BH_4)_2$ for various molar ratios n. It clearly confirms that the contribution from B_2H_6 evolved is negligibly small (if any) when desorption occurs isothermally in the practical temperature range 100–200 °C. It is found that the ball milled mixture with the molar ratio $n = 3$ exhibits the highest rate constant k and the lowest apparent activation energy for dehydrogenation, E_A ~ 102 kJ/mol. Decreasing or increasing the molar ratio n below or

* Corresponding author.
E-mail addresses: ravarin@uwaterloo.ca, ravarin@mecheng1.uwaterloo.ca (R.A. Varin).

http://dx.doi.org/10.1016/j.ijhydene.2012.08.001

above 3 increases the apparent activation energy. Ball milled mixtures with the molar ratio $n = 2$ and 3 discharge slowly H_2 during storage at room temperature and 40 °C. The addition of 5 wt.% nano-Ni with a specific surface area of 60.5 m^2/g substantially enhances the rate of discharge at 40 °C.

1. Introduction

An effective method of solid state hydrogen storage in hydrides and their composites [1] is one of the obstacles in transforming the present fossil fuel based economy to the hydrogen economy. The most important area for transformation from fossil fuels to hydrogen is mass transportation using cars (automotive). A most suitable for the automotive application and many others is a Proton Exchange Membrane (PEM) fuel cell. Due to the specific requirements of a Proton Exchange Membrane (PEM) fuel cell stack, a potential hydride-based storage system should have the operating temperature of dehydrogenation compatible with waste heat of a PEM fuel cell stack which should not exceed 70–100 °C at a feed pressure slightly above 1 bar H_2. The most recently revised US Department of Energy (DOE) automotive hydrogen storage targets for 2015 require H_2 capacity of 5.5 wt.% for the entire storage *system* which includes storage medium, tank and some auxiliary devices [2]. This translates into approximately 10–11 wt.% H_2 capacity for the solid hydride-based storage material. Such large capacities can only be provided by complex light metal/nonmetal hydrides and most likely by their mixtures [1]. In this context, metal borohydrides are potentially interesting solid state hydrogen storage materials due to their very high theoretical capacities of hydrogen [1,3–8]. The most prominent among borohydrides is lithium borohydride ($LiBH_4$) which is easily commercially available and has a theoretical gravimetric hydrogen capacity 18.4 wt.%. Unfortunately, its dehydrogenation is not an easy task due to its relatively high enthalpy change for dehydrogenation which, in turn, results in the dehydrogenation temperatures in excess of 400 °C [3–5]. The addition of metal and non-metal catalysts accelerates the dehydrogenation rate of $LiBH_4$ but does not change its unfavorable thermodynamics [5–8].

Nakamori et al. [9,10] used the mechano-chemical activation synthesis (MCAS) which occurs during high energy ball milling of complex hydrides mixed with appropriate metal di- or tri-chlorides, MCl_n, for synthesizing a large spectrum of metal borohydrides. In essence this is a "metathesis reaction" in solid state instead of the one which uses diethyl ether as a solvent [1]. They used the mixture of metal chlorides MCl_n and both lithium and sodium borohydride, $LiBH_4$ and $NaBH_4$, respectively, which were milled in argon for 5 h. The reaction during milling was proposed to occur as follows:

$$MCl_n + nLiBH_4 \rightarrow M n(BH_4)_n + nLiCl \ (M = Cr, Mg, Mn, Zr, Ti, V, Zn) \quad (1)$$

$$MCl_n + nNaBH_4 \rightarrow M n(BH_4)_n + nNaCl \ (M = Ca, Sc, Al) \quad (2)$$

The post-MCAS XRD patterns for reaction (1) with $LiBH_4$ showed the absence of the diffraction peaks of crystalline $M(BH_4)_n$ and the presence of LiCl peaks. When $NaBH_4$ was used in reaction (2) then only the NaCl peaks were present while the diffraction peaks of $NaBH_4$ were also observed for $NaBH_4$ and MCl_n where M = Ca, Sc and Al mixtures in reaction (2). This very unusual observations were interpreted by Nakamori et al. as evidence of the "disordering" of the crystal structure of $M(BH_4)_n$ although this interpretation is incorrect at least in the case of the ($LiBH_4$–$MnCl_2$) mixture as will be discussed further. Nakamori et al. [9,10] concluded that reaction (1) with $LiBH_4$ occurred easier than reaction (2) with $NaBH_4$ due to similar ionic radii of Li^{1+} and M^{n+} in solid–solid cation exchange reaction as compared to a larger ionic radius of Na^{1+}. Indeed, soon after their reports, Varin et al. [11] reported that the MCAS of the ($2NaBH_4 + MgCl_2$) mixture resulted in only a partial synthesis of "disordered" magnesium borohydride $Mg(BH_4)_2$ accompanied by (Na, Mg)BH_4 solid solution and NaCl which somehow confirms that $NaBH_4$ may not be so effective as $LiBH_4$ in reacting with metal chloride during MCAS. Nakamori et al. [9,10] also reported that the hydrogen desorption temperature of disordered $M(BH_4)_n$ (T_d) decreased with increasing values of the Pauling electronegativity χ_P of metal M in borohydride. They noted that the desorbed gas for M = Ca, Sc, Ti, V and Cr ($\chi_P \leq 1.5$) was hydrogen only, while that for M = Mn, Zn and Al ($\chi_P \geq 1.5$) contained a mix of borane and hydrogen.

In the further development in the field of synthesized metal borohydrides, Choudhury et al. [12] assumed a priori that the MCAS of $LiBH_4$ with $MnCl_2$ in the ratio of 3:1 would result in the formation of new complex metal borohydride $LiMn(BH_4)_3$. They did not observe diffraction peaks other than LiCl and claimed that "disordered" $LiMn(BH_4)_3$ was synthesized. Subsequently, Varin et al. [13] carried out the MCAS on the ($3LiBH_4 + MnCl_2$) also with a presumption that $LiMn(BH_4)_3$ would be synthesized. Beside the LiCl diffraction peaks they observed some unidentified diffraction peaks which were later identified as belonging to $Mn(BH_4)_2$ as it was at the same time reported in [14–16]. Very recently, Liu et al. [17] reported limited studies of thermal decomposition behavior of $LiBH_4$ ball milled with $MnCl_2$ with the molar ratio $n = 2$ and 3. From Differential Scanning Calorimetry (DSC) and TG (thermogravimetric) analysis they deduced that dehydrogenation of $Mn(BH_4)_2$ occurs with the release of diborane (B_2H_6). They didn't conduct any isothermal dehydrogenation tests under 1 bar H_2 pressure.

The present paper is a continuation of studies published in [13] where the MCAS of the ($3LiBH_4 + MnCl_2$) system was studied. In the present work a wide range of molar ratios $n = 1$, 2, 3, 5, 9 and 23 is used in the ($nLiBH_4 + MnCl_2$) mixture. The emphasis is placed on the structural development during MCAS investigated by X-ray and synchrotron diffraction, isothermal volumetric dehydrogenation under 1 bar H_2

pressure including estimates of apparent activation energy and slow hydrogen discharge during storage at room temperature and 40 °C. These aspects were not reported in the previous publications.

2. Experimental

As-received commercial $LiBH_4$ (95% purity) and $MnCl_2$ (99.99% purity) from Alfa Aesar were mixed to the molar ratios ($nLiBH_4 + MnCl_2$) where $n = 1, 2, 3, 5, 9$ and 23. The effect of addition of 5 wt.% catalytic nanometric nickel (n-Ni) produced by Vale Ltd., Mississauga, Ontario, on a slow hydrogen self-discharge during long term storage at low temperatures, as already reported for $LiAlH_4$ [18], was also investigated for one batch with the molar ratio $n = 3$. Two batches of n-Ni with Specific Surface Area (SSA) of 9.5 and 60.5 m^2/g which were measured in the Vale Ltd.'s laboratories by the BET (Brunauer, Emmett and Teller) method were used as possible catalytic additives. Their characteristics and effects on isothermal dehydrogenation of the $n = 3$ composite were already reported in [13].

Controlled Mechanical Milling (CMM) of all mixtures was carried out for 30 min in ultra-high purity hydrogen gas atmosphere (purity 99.999%: $O_2 < 2$ ppm; $H_2O < 3$ ppm; $CO_2 < 1$ ppm; $N_2 < 6$ ppm; CO < 1 ppm; THC < 1 ppm) at ~600 kPa pressure in the magneto-mill Uni-Ball-Mill 5 manufactured by A.O.C. Scientific Engineering Pty Ltd, Australia [1,19–21]. The milling was carried out under a strong impact mode (IMP68) with two magnets positioned at 6 and 8 o'clock, at the distance from the vial of ~10 and ~2 mm, respectively [13]. The ball-to-powder weight ratio (R) was 132 and the rotational speed of milling vial was ~200 rpm. After loading with powder, an air-tight milling vial with an O-ring, equipped with a pressure valve mounted in the lid, was always first evacuated and then purged several times with ultra-high purity argon (Ar) gas (99.999% purity) before final pressurization with H_2. During milling the vial was continuously cooled by an air fan and the milling process was stopped every 10 min for an additional cool off. The release of hydrogen during ball milling was monitored and estimated from the pressure increase in the milling vial measured by a pressure gage using an ideal gas law [1] and expressed in wt.% with respect to the *total* weight of powder sample with the accuracy ±0.1 wt.% H_2.

The powder samples were handled in a glove box containing a moisture-absorbing Drierite granulated compound. Before handling, the glove box was purged a few times with high purity argon gas (99.999% purity) in order to minimize any possible contamination by moisture or oxygen from air.

The hydrogen thermal desorption/absorption was evaluated using a second generation volumetric Sieverts-type apparatus custom-built by A.O.C. Scientific Engineering Pty Ltd., Australia [1]. The details of the measurements can be found in [13]. Sieverts' volumetric dehydrogenation tests were carried out shortly after completion of milling process to avoid a prolonged storage as will be discussed later. The amount of desorbed hydrogen was calculated from the ideal gas law as described in detail in [1] and expressed in wt.% with respect to the *total* weight of powder sample. The calibrated accuracy of desorbed hydrogen capacity is about ±0.1 wt.% H_2 and that of temperature reading and stabilization ±0.1 °C. The apparent activation energy for volumetric hydrogen desorption was estimated from the obtained Sieverts' dehydrogenation curves using the Arrhenius plot of k values with temperature [1]:

$$k = k_o e^{-E_A/RT} \tag{3}$$

where k is the rate of hydrogen desorption (wt.%H_2/s), E_A is the apparent activation energy (kJ/mol), R is the gas constant (8.314472 J/mol K) and T is absolute temperature (K). The rate constant k was determined using the Johnson-Mehl-Avrami-Kolmogorov (JMAK) equation [1]:

$$\alpha = 1 - e^{-(k\cdot t)^{\eta}} \tag{4}$$

where η is the reaction exponent which is related to transformation mechanism and α is the desorption fraction at time t. The standard error for the apparent activation energy estimate is about ~5 kJ/mol. More details on the apparent activation energy measurements can be found in [22–24].

X-ray powder diffraction (XRD) analysis was performed on a Bruker D8 diffractometer using a monochromated CuKα_1 radiation ($\lambda = 0.15406$ nm) produced at an accelerating voltage of 40 kV and a current of 30 mA. The scan range was from $2\theta = \sim 10$ to ~90° and the rate was ~1.2 min^{-1} with a step size of ~0.02. Powder was loaded in a glove box filled with Ar into a home-made environmental brass holder with a Cu/glass plates for powder support. Upper and lower part of the environmental holder is sealed through a soft-rubber O-ring and tightened using threaded steel bolts with nuts. The upper part of the holder contains a Kapton window transmittable to X-rays. For additional confirmation of the phases present synchrotron powder diffraction was used. The data were collected at the Swiss-Norwegian Beam Lines in Grenoble using the radiation wavelength of 0.73065 Å (more details can be found in [14]).

Temperature programmed desorption (TPD) experiments were performed with the use of HTP1-S Sieverts-type apparatus coupled with a quadrupole mass spectrometer (Hiden Inc.). Sample of about 25 mg was loaded into 100 μl (microliters) alumina crucible (with no contact with atmospheric air) to prevent reaction with copper sample holder. During loading procedure each sample was evacuated down to $1–10^{-5}$ mbar pressure. Experiment was carried out under constant helium (99.999% purity) flow of 100 ml/min. Constant heating rate of 2 and ~10 °C/min was used to register desorption spectra containing both hydrogen and diborane (B_2H_6) signal.

3. Results and discussion

3.1. Microstructure of ball milled composites

A number of complex hydrides and their mixtures containing various additives can partially decompose during highly energetic ball milling desorbing varying amounts of hydrogen [24–26]. In order to find out if the ($nLiBH_4 + MnCl_2$) mixture exhibits similar behavior the pressure change in the milling

vial was continuously monitored during the entire length of the milling process and then converted to wt.% H_2 as mentioned earlier. Fig. 1 shows a trend of increasing amount of desorbed H_2 with increasing molar ratio n of $LiBH_4$ in the mixture during high energy ball milling for 30 min. The amount of H_2 desorbed during 30 min of ball milling even for the $n = 23$ mixture is still very small and does not exceed 0.2 wt.% which is close to the experimental error of measurements. However, when the milling duration was extended to 1 h for the ($3LiBH_4 + MnCl_2$) molar ratio then the H_2 desorption was more substantive reaching about 1 wt.% after completion of milling. Therefore, it is not recommended to exceed 30 min of mechanical milling for which in all practical terms the mechanical dehydrogenation phenomenon can be neglected. We are now investigating the mechanical dehydrogenation phenomenon for $Mn(BH_4)_2$ and other complex hydrides in more detail.

Fig. 2a and b shows X-ray and synchrotron diffraction pattern, respectively, for mixtures with varying molar ratio n after high energy ball milling. The X-ray results which are supported by the synchrotron results clearly show that in all mixtures the $Mn(BH_4)_2$ hydride has been synthesized by the mechano-chemical "metathesis" reaction. The identification of this hydride was based on data reported in [14–16] which show that $Mn(BH_4)_2$ has a hexagonal lattice structure with $a = 10.435(1)$ Å and $c = 10.835(2)$ Å.

However, depending on the exact value of the molar ratio n there are some differences with respect to the presence of other phases after ball milling. A majority phase in the equimolar $n = 1$ mixture is an inverse cubic spinel phase Li_2MnCl_4 (file # 1984-ICSD) while a minority phase is $Mn(BH_4)_2$. It should also be noted that Li_2MnCl_4 has its diffraction peaks shifted to slightly bigger d-values which suggests that there is a solid solution between Cl and BH_4 anions. This spinel has been extensively studied for its ionic conductivity as a potential solid electrolyte for lithium-ion batteries [27–29]. The present work clearly shows that this important compound can be relatively easily synthesized by ball milling.

For $n = 2$ the pattern is changed where instead of Li_2MnCl_4 a LiCl salt appears. The presence of the latter was also proposed by Nakamori et al. [9,10]. Obviously, a minority phase in the $n = 2$ mixture is $Mn(BH_4)_2$. With the n increasing from 3 to 23 both XRD and synchrotron patterns (Fig. 2a and b) show steadily increasing intensity of $LiBH_4$ diffraction peaks.

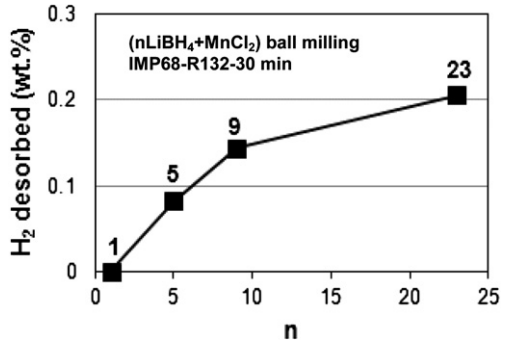

Fig. 1 – The amount of H_2 desorbed during high energy ball milling for 30 min of ($nLiBH_4 + MnCl_2$) vs. the molar ratio n.

This confirms that $LiBH_4$ is not completely reacted and an increasing amount of $LiBH_4$ is retained in the microstructure. The identification of $LiBH_4$ peaks was based on our own standard XRD pattern for ball milled $LiBH_4$ compared with a diffraction pattern reported in [30]. Therefore, the results of diffraction studies in Fig. 2a and b clearly indicate that the reaction paths in the mechano-chemical metathesis depend on the molar ratio n of $LiBH_4$ to $MnCl_2$ according to the following reactions:

$$LiBH_4 + MnCl_2 \rightarrow 0.5Mn(BH_4)_2 + 0.5Li_2MnCl_4 \quad (n = 1) \tag{5}$$

$$nLiBH_4 + MnCl_2 \rightarrow Mn(BH_4)_2 + 2LiCl + (n-2)LiBH_4 \quad (n = 2–23) \tag{6}$$

3.2. *Thermal behavior*

Fig. 3 shows TPD gas desorption spectra combined with a mass spectroscopy analysis for ball milled $n = 3$ (Fig. 3a and b) and $n = 5$ mixtures (Fig. 3c and d), for two heating rates of 2 °C/min and 10 °C/min. The primary H_2 release peak from $Mn(BH_4)_2$ is centered around 130–150 °C depending on the heating rate. The second smaller and very broad H_2 release peak occurs in a wide temperature range 300–450 °C. This second peak corresponds to the decomposition of retained $LiBH_4$ which is a very volatile process as evidenced by sharp random peaks appearing at 300–450 °C in Fig. 3c and d for the $n = 5$ mixture which are related to the melting of excess $LiBH_4$. In Fig. 3a around 130 °C there is also a miniscule peak corresponding to the release of diborane B_2H_6. The intensity of the borane peak increases with increasing heating rate from 2 to 10 °C/min (Fig. 3b). For $n = 5$ at the heating rate 2 °C/min the B_2H_6 peak does not appear (Fig. 3c) while it re-appears again when the heating rate increases to 10 °C/min (Fig. 3d). It seems that B_2H_6 is released in the gas mixture with H_2 only at higher heating rates and for low molar ratios $n \leq 5$ although this phenomenon should be studied more thoroughly to arrive at a definite conclusion. Furthermore, the intensity of the B_2H_6 peak even if it is observed is 200–600 times smaller than the intensity of the corresponding H_2 peak. The obtained results mean that the quantity of released diborane is miniscule being barely on the verge of the resolution of the Hiden Sieverts apparatus-quadrupole mass spectrometric experimental system. It must be pointed out that Liu et al. [17] reported that the relatively low intensity of diborane peaks they observed in their thermogravimetric experimental set up was due to the fact that large quantities of diborane did not reach the mass spectrometer. They observed some borate deposits on the piping system. They measured a high mass loss of 8.4 wt.% which possibly indicated a release of diborane. However, this is not the case in the present work as will be shown later.

Therefore, in accord with the gas thermal analysis results obtained in this work the decomposition reaction of $Mn(BH_4)_2$ can be written as follows neglecting minutiae quantities of B_2H_6 (if any):

$$Mn(BH_4)_2 \rightarrow Mn + 2B + 4H_2 \tag{7}$$

Our mass spectroscopy results of released gas are in agreement with Choudhury et al. [12] who reported that for

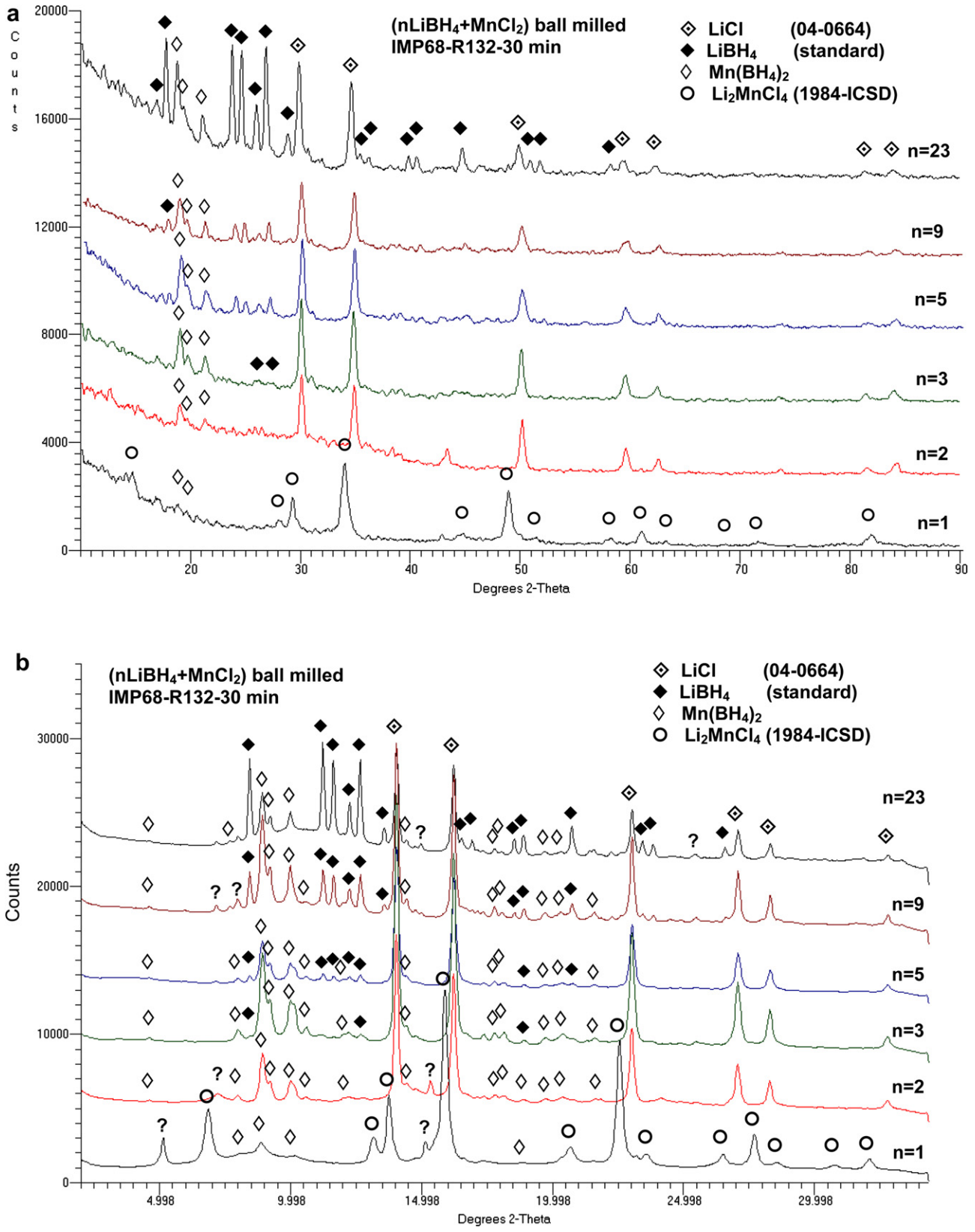

Fig. 2 – (a) X-ray diffraction pattern and (b) synchrotron diffraction pattern (the radiation wavelength $\lambda = 0.73065$ A) for the ($nLiBH_4 + MnCl_2$) mixtures where $n = 1, 2, 3, 5, 9$ and 23, synthesized for 30 min by mechano-chemical synthesis under high energy impact milling mode (IMP68). ICDD and ICSD file numbers for peak identification of LiCl and Li_2MnCl_4 are shown in the legend.

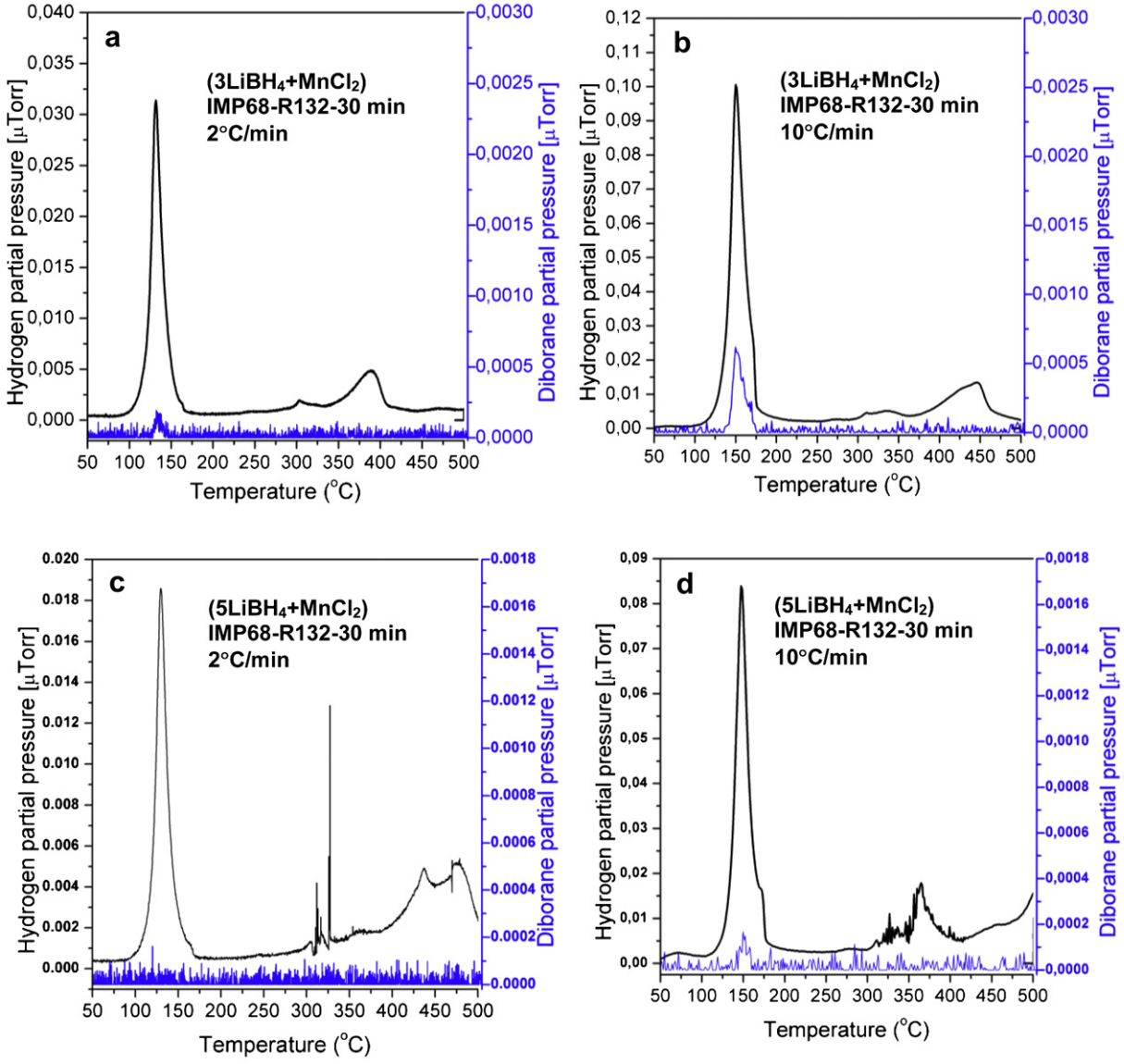

Fig. 3 – TPD gas desorption spectra for a mixture with (a, b) $n = 3$ and (c, d) $n = 5$ at two heating rates of 2 °C/min and 10 °C/min.

a ball milled ($3LiBH_4 + MnCl_2$) mixture a gas chromatography analysis showed only H_2 desorbed without any other gases upon repeated sampling.

As mentioned above, decomposition of retained $LiBH_4$ also occurs at the 350–450 °C range but it has no practical meaning due to very high temperatures involved.

We also investigated melting behavior of the $n = 2$ and 3 ball milled mixtures. According to reactions (6) and (7) after completion of ball milling the $n = 2$ and 3 mixture consists of ($Mn(BH_4)_2 + LiCl$) and ($Mn(BH_4)_2 + LiCl + LiBH_4$), respectively. A small amount of mixture powder was placed on a pure copper button which, in turn, was placed on a hot plate. A thermocouple was attached to the copper button. This experimental set up was located in a glove box which was purged several times using high purity argon gas. The temperature was slowly increased to 274 and 286 °C for the $n = 2$ and 3 mixture, respectively. The behavior of powder was continuously filmed with a digital camera during heating. No evidence of melting of $Mn(BH_4)_2$ was observed. We only observed that the milled powder changed its color from gray to black most likely due to a local sintering. After heating the powder was slightly sintered but it could be easily broken loose into a fine dry powder. Černý et al. [14] reported that in a mixture with LiCl the $Mn(BH_4)_2$ hydride melted at about 177 °C (450 K). Apparently, the present experiments do not confirm such a low melting temperature of $Mn(BH_4)_2$ which is observed to be stable at least up to about 270–280 °C.

3.3. *Isothermal dehydrogenation*

Fig. 4 shows the examples of isothermal dehydrogenation curves at temperatures from 100 °C to 200 °C in 1 bar H_2

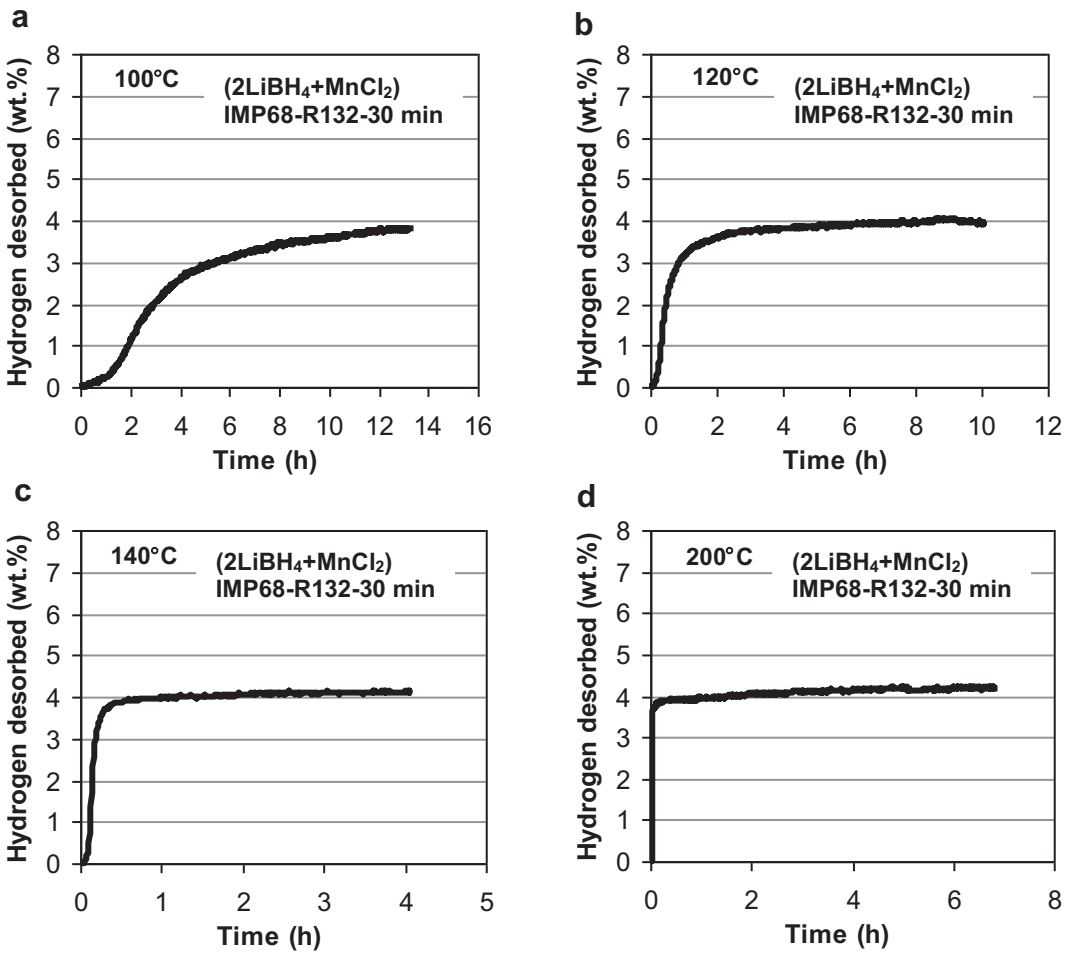

Fig. 4 – Examples of isothermal volumetric dehydrogenation curves at (a) 100 °C, (b) 120 °C, (c) 140 °C and (d) 200 °C, under 1 bar H_2 pressure for the ball milled ($2LiBH_4 + MnCl_2$) mixture.

pressure for the ball milled ($2LiBH_4 + MnCl_2$) mixture. It can be seen that the $n = 2$ mixture containing $Mn(BH_4)_2$ and 2LiCl after synthesis desorbs quite rapidly about 4 wt.% H_2 at 100 °C under 1 bar H_2 pressure (Fig. 4a). This quantity of desorbed H_2 is not measurably changed during desorption up to 200 °C (Fig. 4b–d). The desorbed H_2 quantity is nearly a half of $Mn(BH_4)_2$ theoretical H_2 capacity which is, indeed, a very large quantity of desorbed H_2, keeping in mind that the ball milled mixture contains 2 mol of LiCl (Eq. (6)) which is simply a "dead-weight". As mentioned in [13] a complete removal of LiCl from the microstructure could be achieved in the well-known Soxhlet extractor which was already successfully used for extracting LiCl and NaCl from solid mixtures with alanates [31,32]. Such an additional LiCl extraction processing could definitely substantially boost the H_2 desorption capacity from a nearly single-phase $Mn(BH_4)_2$ having a theoretical capacity of 9.5 wt.% H_2 for the composites with $n = 2$ and 3 molar ratios.

Table 1 – The H_2 quantities experimentally desorbed at 100 and 200 °C from $Mn(BH_4)_2$ ball milled for 30 min for various molar ratios n as compared to the theoretical quantities of H_2 calculated according to reaction (6).

Molar ratio n	Mole $Mn(BH_4)_2$ after ball milling	No. moles H from reaction (7)	Molar mass H from reaction (7) (g/mol)	Molar mass ($nLiBH_4 + MnCl_2$) (g/mol)	Theoretical H_2 content from reaction (7) (wt.%)	Experimental hydrogen desorbed at 100 and 200 °C (wt.%)
1	0.5	4	4.032	147.628	2.73	0.9 and 2.4
2	1.0	8	8.064	169.412	4.76	3.8 and 4.2
3	1.0	8	8.064	191.196	4.22	4.2 and 4.5
5	1.0	8	8.064	234.764	3.43	2.6 and 2.7
9	1.0	8	8.064	321.900	2.50	2.1 and 2.2
23	1.0	8	8.064	626.876	1.29	1.3 and 1.3

Note: Molar masses (g/mol) taken for computing are as follows: H = 1.008; Li = 6.941; B = 10.811; Mn = 54.938; Cl = 35.453.

Even without catalytic additives, the rate of dehydrogenation in Fig. 4 is very reasonable since 4 wt.% H_2 can be obtained within about 12 h at 100 °C (Fig. 4a). At only slightly higher temperature of 120 °C the dehydrogenation time for the same quantity of H_2 is reduced by half to just 4–6 h (Fig. 4b) and is proportionally shorter at 140 and 200 °C.

Table 1 shows the H_2 quantities experimentally desorbed at 100 and 200 °C compared to the maximum theoretical

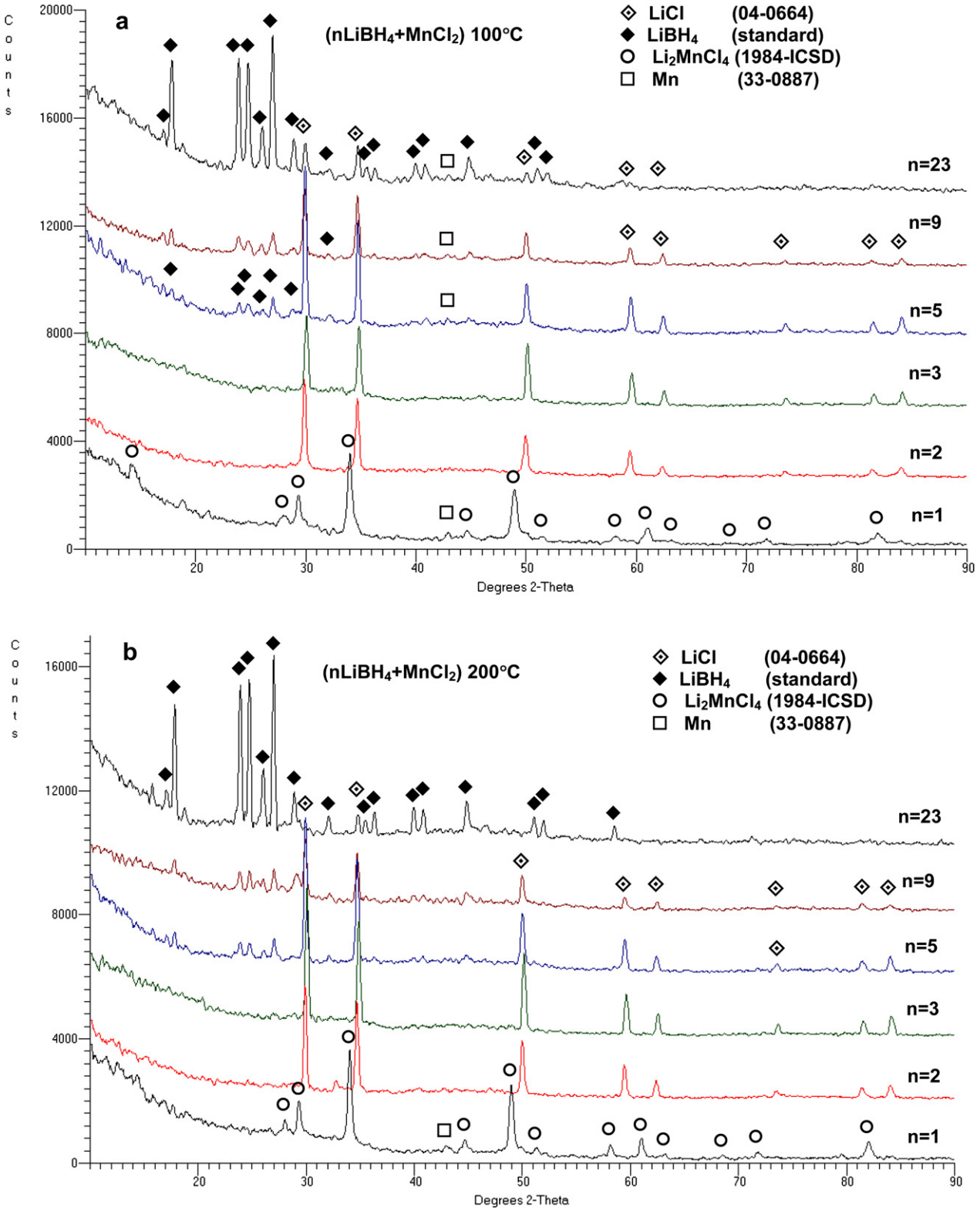

Fig. 5 – XRD patterns for all mixtures after full dehydrogenation at (a) 100 °C and (b) 200 °C. ICDD and ICSD file numbers for peak identification of LiCl, Li_2MnCl_4 and Mn are shown in the legend.

quantities of H_2 expected to be desorbed from $Mn(BH_4)_2$ for various molar ratios n calculated according to reaction (7). It is observed that at 100 and 200 °C the quantities of H_2 desorbed from $Mn(BH_4)_2$ do not exceed the theoretical H_2 quantities expected to be desorbed from a mixture with n = const according to reaction (7). It clearly confirms the fact, already observed in Fig. 3, that the contribution from B_2H_6 is negligibly small (if any) when desorption occurs isothermally in the practical temperature range 100–200 °C. As mentioned above, Liu et al. [17] proposed that a decomposition of $Mn(BH_4)_2$ could occur via formation of B_2H_6 according to the following reaction:

$$Mn(BH_4)_2 \rightarrow Mn + H_2 + B_2H_6 \quad (8)$$

However, reaction (8) requires that the quantities of desorbed (H_2 + B_2H_6) gas to be several times larger than those experimentally observed in the present work as listed in Table 1. The obtained results allow us to conclude that the isothermal dehydrogenation of $Mn(BH_4)_2$ mechano-chemically synthesized by ball milling occurs at the temperature range of 100–200 °C (under 1 bar H_2 pressure) without a measurable contribution from B_2H_6 according to reaction (7) rather than reaction (8).

In order to monitor the microstructural evolution occurring during isothermal dehydrogenation the XRD tests were carried out on mixtures fully desorbed at 100 °C (Fig. 5a) and 200 °C (Fig. 5b). Full desorption means that dehydrogenation was carried out to the end of each desorption curve in Fig. 4. The peaks of Li_2MnCl_4, LiCl and $LiBH_4$ remain essentially unchanged after desorption by comparison with their counterparts for the ball milled structure in Fig. 2a. The peaks of $Mn(BH_4)_2$ disappeared. Very weak peaks of Mn appear on a few but not all XRD patterns indicating that Mn could be partially crystalline and possibly partially amorphous. The microstructure observed after desorption is in a qualitative agreement with reaction (7) occurring during dehydrogenation. No peaks of crystalline B from reaction (7) are present after dehydrogenation which indicates that B must be fully amorphous.

The apparent activation energy was estimated and the examples of the Arrhenius plots of rate constant k with temperature according to Eq. (3) for the mixtures with the molar ratios n = 1, 2, 3 and 5 are presented in Fig. 6a–d, respectively. Corresponding temperatures for which estimates were done are also shown in the plots. Excellent coefficients of fit R^2 give a testimony to the accuracy of the method. Fig. 7a shows a plot of rate constant k in Eq. (3) vs. the molar ratio n for all ball milled mixtures, calculated for dehydrogenation at 120 °C. It is observed that the k values achieve a maximum for n = 3. Correspondingly, Fig. 7b shows that the apparent activation energy for dehydrogenation plotted vs. the molar ratio n, exhibits a minimum value of ~102 kJ/mol for n = 3. This value was already reported by Varin et al. [13] and it was also reported that the apparent activation energy was reduced to ~92 kJ/mol with added 5 wt.% nanometric Ni having SSA = 60.5 m^2/g [13].

With the molar ratio $n < 3$ and $n > 3$ the apparent activation energy for the $Mn(BH_4)_2$ dehydrogenation is larger than that for n = 3. This effect is very pronounced in Fig. 7b. According to reaction (7) for a mixture having n = 3 a small quantity of $LiBH_4$ is retained after mechano-chemical synthesis while there is no retained $LiBH_4$ for $n < 3$ and the $LiBH_4$ quantity increases for $n > 3$. It is hypothesized that that a small quantity of retained $LiBH_4$ may accelerate the hydrogen desorption rate from

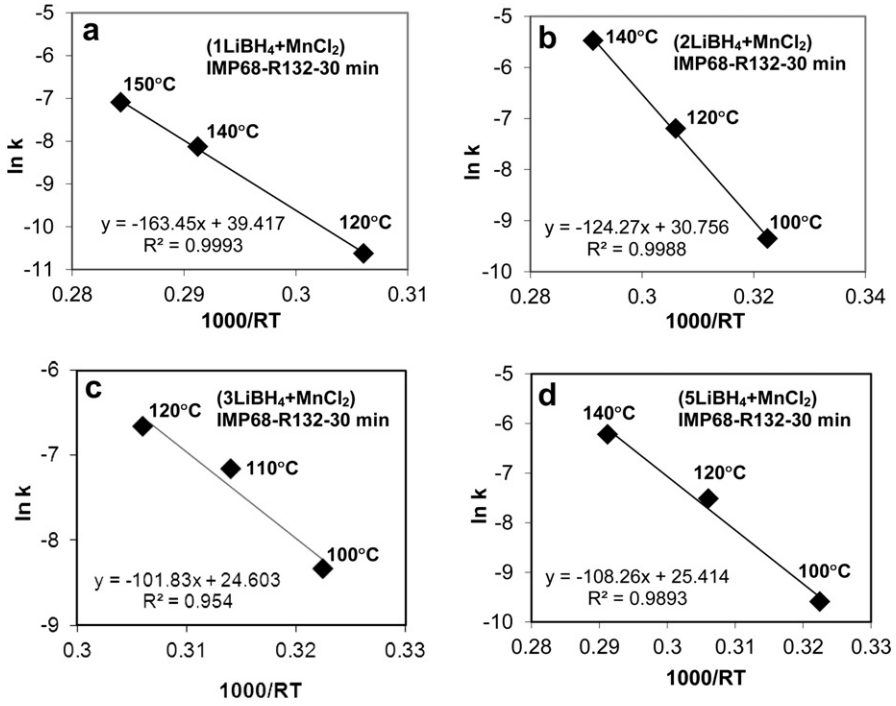

Fig. 6 – Examples of the Arrhenius plots of rate constant k with temperature for estimation of the apparent activation energy of hydrogen desorption for the mechano-chemically synthesized ($nLiBH_4$ + $MnCl_2$) mixtures. (a) n = 1, (b) n = 3, (c) n = 3 and (d) n = 5. The three temperatures used for each plot are shown.

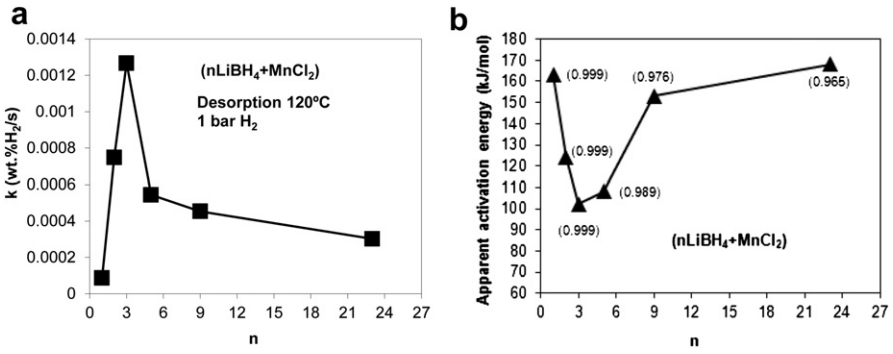

Fig. 7 – (a) The rate constant *k* in Eq. (3) plotted vs. the molar ratio *n* for 120 °C and (b) the estimated apparent activation energy vs. the molar ratio *n* for ball milled ($nLiBH_4 + MnCl_2$) mixtures. Coefficients of fit R^2 are shown in parentheses.

$Mn(BH_4)_2$ whereas both decrease and increase in the quantity of retained $LiBH_4$ with decreasing/increasing *n* eliminates this effect. However, the exact atomistic mechanism is not clear at the moment. Apparently, the mixture with $n = 3$ exhibits the highest rate constant *k* and correspondingly the lowest apparent activation energy. This is a very interesting results showing that the molar ratio $n = 2$ may not be the optimal one.

So far, the only paper reporting the apparent activation energy of dehydrogenation for $Mn(BH_4)_2$ is published by Choudhury et al. [12] for the ball milled ($3LiBH_4 + MnCl_2$) mixture. For the undoped system they report the value of 130.6 kJ/mol. This value is higher than ~102 kJ/mol obtained in [13] and the present work. However, Choudhury et al. used the Kissinger plots from the TPD data for their assessment of the apparent activation energy in contrast to the JMAK/Arrhenius method used in the present work for the direct volumetric hydrogen desorption data. We have found that these two diverse methodologies can give results differing within a 10–20% range.

3.4. *Self-discharge of hydrogen at low temperatures*

Recently, it has been reported for the first time by Varin et al. that a few ball milled $LiAlH_4$-based mixtures combined with nanometric-size metal catalysts [18,24], complex hydride $LiNH_2$ [25] and a $MnCl_2$ catalytic precursor [33] continuously self-discharge H_2 when stored for a prolonged time in glass vials at a temperature range from room temperature (RT) to 80 °C under slight overpressure of high purity argon. In order to find out if the same phenomenon occurs for the present ($nLiBH_4 + MnCl_2$) mixtures, first of all, a ball milled ($2LiBH_4 + MnCl_2$) mixture, which according to reaction (6) and Fig. 2a contains $Mn(BH_4)_2$ and 2 mol of LiCl, was dehydrogenated in a Sieverts-type apparatus at 100 °C under 1 bar H_2 pressure immediately after ball milling (0 days storage) and after storage for 11 days at RT under a slight overpressure of high purity argon. The pertinent desorption curves are shown in Fig. 8. It is clearly seen that the desorption curve after 11 days of storage shows a capacity deficiency of about 1.2 wt.% H_2 with respect to the desorption curve obtained immediately after ball milling. Apparently, the $Mn(BH_4)_2$ hydride present in this composite slowly desorbed that quantity of H_2 within 11 days of storage.

Further studies of this phenomenon were conducted on the ball milled ($3LiBH_4 + MnCl_2$) mixture which according to reaction (6) and Fig. 2a contains mainly $Mn(BH_4)_2$, 2 mol LiCl and 1 mol of retained $LiBH_4$. Following procedures reported in [18,24,33] after a pre-determined length of time small samples stored at RT and 40 °C were extracted from the vial and fully dehydrogenated isothermally at a temperature of 140 °C in a Sieverts-type apparatus under 1 bar H_2 pressure, registering the quantity of H_2 desorbed. It was already reported in [13] that the addition of nanometric Ni (n-Ni) to ($3LiBH_4 + MnCl_2$) slightly accelerated dehydrogenation and reduced the apparent activation energy for dehydrogenation. In order to investigate the effect of nano-metal catalyst on the slow self-discharge during storage two batches of nanometric nickel (n-Ni) catalytic additive used in [13], having Specific Surface Area (SSA) = 9.5 and 60.5 m^2/g, were incorporated in the quantity of 5 wt.% into ($3LiBH_4 + MnCl_2$) by ball milling.

Fig. 9 shows the quantities of H_2 desorbed at 140 °C after long storage at room temperature (RT) and 40 °C of samples without and with the catalytic additive of nanometric Ni (n-Ni). It is seen in Fig. 9a and b that the $n = 3$ mixture without any additive discharges only a small amount of ~0.7 and 1.4 wt.% H_2 after storage for 70–80 days at RT and 40 °C, respectively. The addition of n-Ni does not measurably change the rate of self-discharge at RT (Fig. 9c and e) although the n-Ni additive

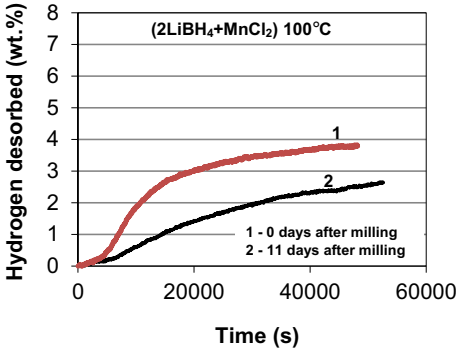

Fig. 8 – Dehydrogenation curves at 100 °C at 1 bar H_2 pressure for the ball milled ($2LiBH_4 + MnCl_2$) mixtures immediately after ball milling (curve 0 days) and after 11 days of storage in a glass vial under high purity argon (curve 11 days).

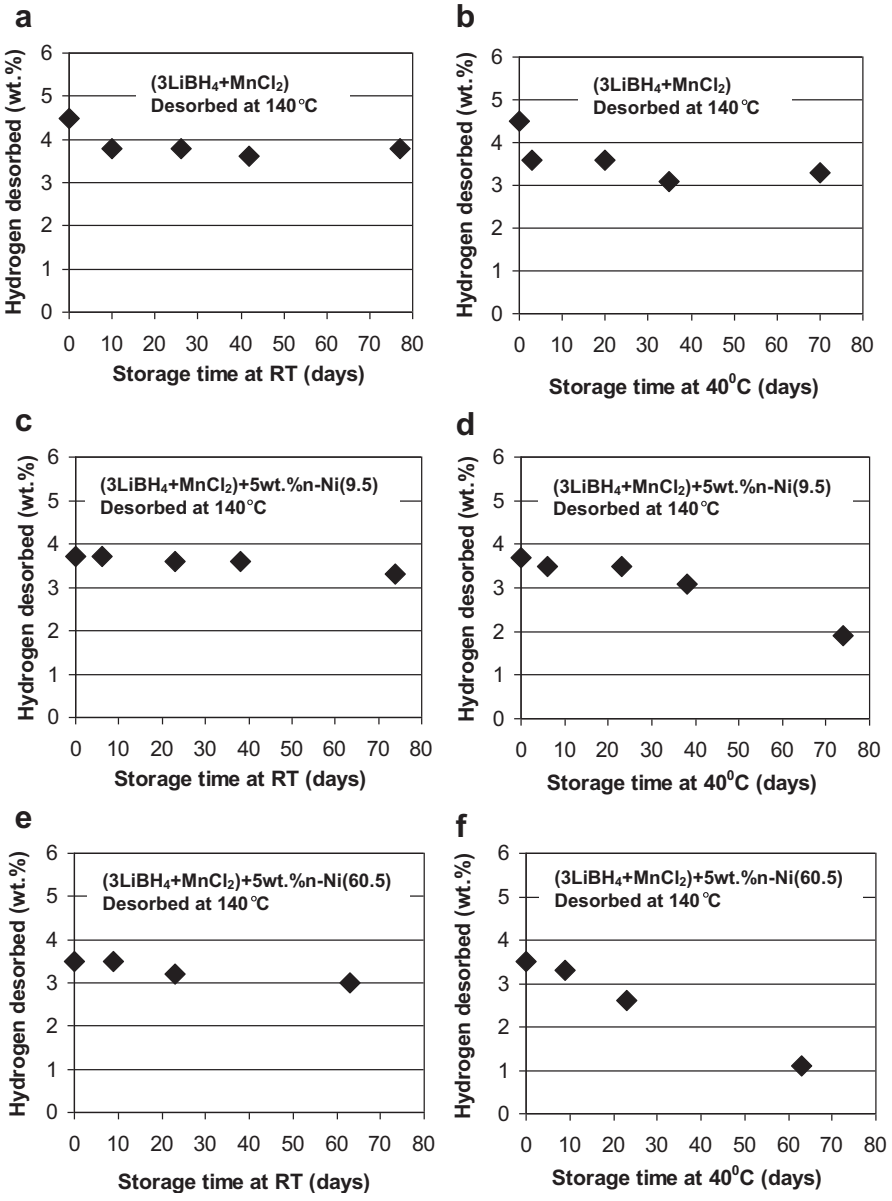

Fig. 9 – The quantities of hydrogen desorbed at 140 °C in 1 bar H_2 pressure after long term storage of ball milled ($3LiBH_4 + MnCl_2$)(microstructure consisting of $Mn(BH_4)_2 + 2LiCl + LiBH_4$) at low temperatures. (a) No additive; stored at room temperature (RT), (b) no additive; stored at 40 °C, (c) with 5 wt.% n-Ni SSA = 9.5 m^2/g; stored at RT, (d) with 5 wt.% n-Ni SSA = 9.5 m^2/g; stored at 40 °C, (e) with 5 wt.% n-Ni SSA = 60.5 m^2/g; stored at RT and (f) with 5 wt.% n-Ni SSA = 60.5 m^2/g; stored at 40 °C. SSA-specific surface area. Storage in a glass vial under high purity argon.

visibly accelerates it at 40 °C (Fig. 9d and f). Particularly effective is n-Ni with SSA = 60.5 m^2/g which allows discharge of ~2.5 wt.% H_2 within 63 days of storage at 40 °C (Fig. 9f). However, it should be pointed out that the rates of H_2 self-discharge observed for $LiAlH_4$ ball milled with nanometric Ni and Fe additives reported in [18,24] are much higher than that for ball milled ($3LiBH_4 + MnCl_2$) containing n-Ni with SSA = 60.5 m^2/g in the present work. By comparison, at a 40 °C storage temperature ($LiAlH_4$ + 5 wt.% n-Ni/n-Fe) discharged about 4.7 wt.% H_2 during 20 days of storage and then saturated at longer storage times [18,24].

Fig. 10 shows a comparison of the XRD pattern for as-milled ($3LiBH_4 + MnCl_2$)(a phase mixture of $Mn(BH_4)_2 + 2LiCl + LiBH_4$) containing n-Ni with SSA = 60.5 m^2/g and the XRD pattern of the same mixture after storage for 95 days at 40 °C (~2.5 wt.% H_2 discharged). In the ball milled sample the diffraction peaks of $Mn(BH_4)_2$ are well developed whereas in the sample stored for 95 days the $Mn(BH_4)_2$ peaks are more diffuse and their intensity is reduced. A clear peak of Mn is also observed. This confirms that $Mn(BH_4)_2$ was gradually decomposing as experimentally observed by the H_2 release according to reaction (7) without any release of B_2H_6. Since no peaks of crystalline B are observed, which is required by reaction (7), it is most likely that B is in an amorphous state.

Finally, it should be pointed out that a phenomenon of H_2 self-discharge from hydride composites during their storage

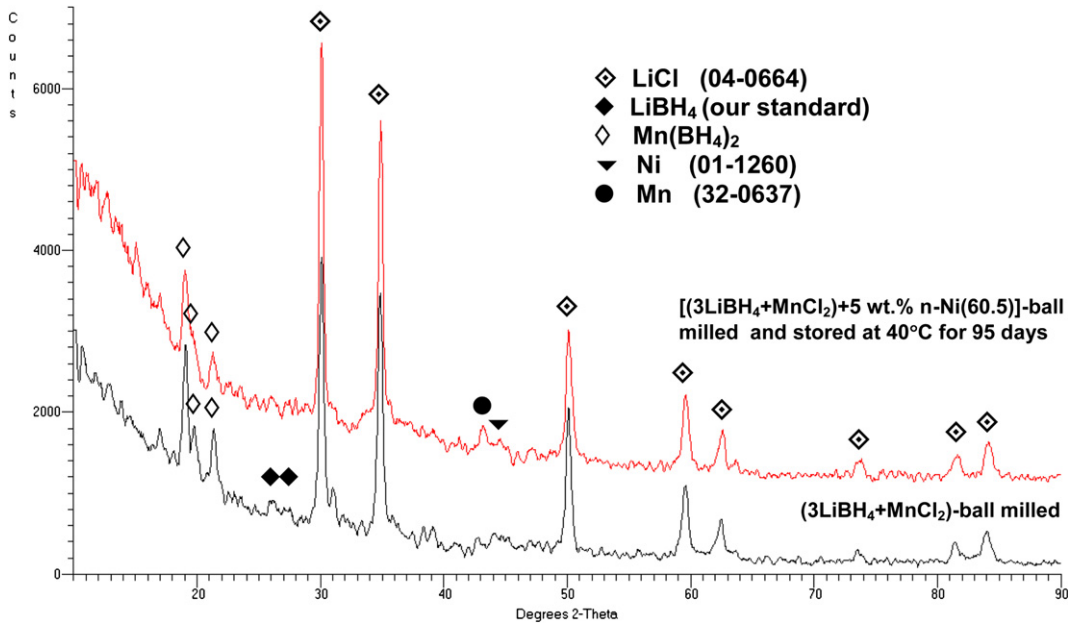

Fig. 10 – XRD patterns for ($3LiBH_4 + MnCl_2$) ball milled and the mixture after 95 days of storage at room temperature (RT) in a glass vial under high purity argon. ICDD file numbers for peak identification are shown in the legend.

at low temperatures is not only very interesting scientifically but also has some practical implications. Sandrock et al. [34,35] pointed out the significance of such a behavior for long-duration, low-demand devices that use H_2 such as low power remote fuel cells or portable gas analyzers. Materials slowly discharging H_2 can also be used in a number of chemical processes where a continuously reducing atmosphere is needed for a completion of the process. They can also have an application in a military sector for long-term cartridges supplying hydrogen to portable devices for soldiers on a mission.

4. Conclusions

The present paper reports the results of the mechano-chemical activation synthesis (MCAS) of manganese borohydride ($Mn(BH_4)_2$) from mixtures of lithium borohydride ($LiBH_4$) and manganese chloride ($MnCl_2$) and its thermal dehydrogenation behavior. For the first time a wide range of molar ratios $n = 1$, 2, 3, 5, 9 and 23 is used in the ($nLiBH_4 + MnCl_2$) mixtures. The main conclusions can be summarized as follows:

(1) During ball milling up to 30 min the ($nLiBH_4 + MnCl_2$) mixtures desorb very small quantities of H_2 which increase with increasing molar ratio n but do not exceed 0.2 wt.% even for $n = 23$. However, when the milling duration was extended to 1 h for the ($3LiBH_4 + MnCl_2$) mixture then the H_2 desorption was more substantive reaching about 1 wt.% after completion of milling.

(2) XRD and synchrotron diffraction studies confirm that for the molar ratio $n = 1$ the principal phases synthesized by the MCAS are Li_2MnCl_4 (cubic spinel) and $Mn(BH_4)_2$ according to following reaction: $LiBH_4 + MnCl_2 \rightarrow 0.5Mn(BH_4)_2 + 0.5Li_2MnCl_4$. For $n = 2$ a LiCl salt and $Mn(BH_4)_2$ are formed according to following reaction: $2LiBH_4 + MnCl_2 \rightarrow Mn(BH_4)_2 + 2LiCl$. With the n increasing from 3 to 23, $LiBH_4$ is not completely reacted and its increasing amount is retained in the microstructure coexisting with LiCl and $Mn(BH_4)_2$ according to following reaction: $nLiBH_4 + MnCl_2 \rightarrow Mn(BH_4)_2 + 2LiCl + (n-2)LiBH_4$.

(3) Mass spectrometry of evolving gas during TPD tests shows a strong H_2 release peak and a miniscule borane (B_2H_6) peak at around 150 °C with the intensity of the borane peak being 200–600 times smaller than the intensity of the corresponding H_2 peak.

(4) In situ continuous heating experiments confirm that no evidence of melting of $Mn(BH_4)_2$ is observedat least up to ~280 °C.

(5) Volumetric dehydrogenation tests show that the ($nLiBH_4 + MnCl_2$) mixture with the molar ratios $n = 2$ and 3 consisting mostly of $Mn(BH_4)_2$ and LiCl desorb quite rapidly about 4 wt.% H_2 at 100 °C under 1 bar H_2 pressure. This quantity of desorbed H_2 is not measurably changed during desorption up to 200 °C. This is a very large quantity of desorbed H_2 considering the presence of LiCl dead-weight in the microstructure. It suggests that after extraction of LiCl a single-phase $Mn(BH_4)_2$ would be able to desorb about 9 wt.% H_2 at a 100–200 °C temperature range.

(6) Evolving gas mass spectrometry analysis and volumetric dehydrogenation tests show quite convincingly that the decomposition of $Mn(BH_4)_2$ occurs at the temperature range 100–200 °C with a non-existent or negligibly small contribution from borane gas (B_2H_6).

(7) The ball milled mixture with $n = 3$ exhibits the highest rate constant k and the lowest apparent activation energy for dehydrogenation, $E_A \sim 102$ kJ/mol. Decreasing or increasing the molar ratio n below or above 3 increases the apparent activation energy.

(8) Ball milled $n = 2$ and 3 mixtures discharge slowly H_2 during storage at room temperature and 40 °C. The addition of 5 wt.% nano-Ni with a specific surface area of 60.5 m^2/g substantially enhances the rate of discharge at 40 °C.

Acknowledgments

This research was supported by the NSERC Hydrogen Canada (H2CAN) Strategic Research Network and NSERC Discovery grants which are gratefully acknowledged. The authors acknowledge SNBL at the ESRF for the synchrotron beam time allocation. The authors also thank Dr. Vladimir Paserin and Mr. Steve Baksa of Vale Ltd. (formerly Vale Inco) for producing and supplying the nanometric Ni powders used in this study. The authors are grateful to Prof. Linda Nazar from the Department of Chemistry, University of Waterloo, for allowing access to XRD equipment. Gas mass spectrometry tests were carried out under the supervision of Prof. J. Bystrzycki from the Faculty of New Technologies and Chemistry, Military University of Technology, Warsaw, Poland and financially supported from the Polish Ministry of Sciences and Higher Education, Key Project POIG.01.03.01-14-016/08.

REFERENCES

[1] Varin RA, Czujko T, Wronski ZS. Nanomaterials for solid state hydrogen storage. New York, NY: Springer Science, Business Media; 2009.
[2] Dillich S. DOE hydrogen program 2009 annual progress report, IV.0 hydrogen storage sub-program overview; May 2009.
[3] Züttel A, Rentsch S, Fischer P, Wenger P, Sudan P, Mauron Ph, et al. Hydrogen storage properties of $LiBH_4$. J Alloys Compd 2003;356–357:515–20.
[4] Orimo S, Nakamori Y, Kitahara G, Miwa K, Ohba N, Towata S, et al. Dehydriding and rehydriding reactions of $LiBH_4$. J Alloys Compd 2005;404–406:427–30.
[5] Li H-W, Yan Y, Orimo S-I, Züttel A, Jensen CM. Recent progress in metal borohydrides for hydrogen storage. Energies 2011;4:185–214.
[6] Xia GL, Guo YH, Wu Z, Yu XB. Enhanced hydrogen storage performance of $LiBH_4$–Ni composite. J Alloys Compd 2009; 479:545–8.
[7] Wellons MS, Berseth PA, Zidan R. Novel catalytic effects of fullerene for $LiBH_4$ hydrogen uptake and release. Nanotechnology 2009;20:204022 (4pp).
[8] Zhang BJ, Liu BH. Hydrogen desorption from $LiBH_4$ destabilized by chlorides of transition metal Fe, Co, and Ni. Int J Hydrogen Energy 2010;35:7288–94.
[9] Nakamori Y, Miwa K, Ninomiya A, Li H-W, Ohba N, Towata S, et al. Correlation between thermodynamical stabilities of metal borohydrides and cation electronegativities: first principle calculations and experiments. Phys Rev B 2006;74:045126. 1–9.
[10] Nakamori Y, Li H-W, Kikuchi K, Aoki M, Miwa K, Towata S, et al. Thermodynamical stabilities of metal-borohydrides. J Alloys Compd 2007;446–447:296–300.
[11] Varin RA, Chiu Ch, Wronski ZS. Mechano-chemical activation synthesis (MCAS) of disordered $Mg(BH_4)_2$ using $NaBH_4$. J Alloys Compd 2008;462:201–8.
[12] Choudhury P, Srinivasan SS, Bhethanabotla VR, Goswami Y, McGrath K, Stefanakos EK. Nano-Ni doped Li–Mn–B–H system as a new hydrogen storage candidate. Int J Hydrogen Energy 2009;34:6325–34.
[13] Varin RA, Zbroniec L. The effects of ball milling and nanometric nickel additive on the hydrogen desorption from lithium borohydride and manganese chloride ($3LiBH_4 + MnCl_2$) mixture. Int J Hydrogen Energy 2010;35:3588–97.
[14] Černý R, Penin N, Hagemann H, Filinchuk Y. The first crystallographic and spectroscopic characterization of a 3d-metal borohydride: $Mn(BH_4)_2$. J Phys Chem C 2009;113: 9003–7.
[15] Severa G, Hagemann H, Longhini M, Kaminski JW, Wesolowski TA, Jensen CM. J Phys Chem C 2010;114: 15516–21.
[16] Černý R, Penin N, D'Anna V, Hagemann H, Durand E, Růžička J. $Mg_xMn_{(1-x)}(BH_4)_2$ ($x = 0$–0.8), a cation solid solution in a bimetallic borohydride. Acta Materialia 2011;59:5171–80.
[17] Liu R, Reed D, Book D. Decomposition behaviour of $Mn(BH_4)_2$ formed by ball-milling $LiBH_4$ and $MnCl_2$. J Alloys Compd 2012; 515:32–8.
[18] Varin RA, Zbroniec L. The effects of nanometric nickel (n-Ni) catalyst on the dehydrogenation and rehydrogenation behavior of ball milled lithium alanate ($LiAlH_4$). J Alloys Compd 2010;506:928–39.
[19] Calka A, Radlinski AP. Universal high performance ball-milling device and its application for mechanical alloying. Mater Sci Eng A 1991;134:1350–3.
[20] Patents: WO9104810, US5383615, CA2066740, EP0494899, AU643949.
[21] Calka A, Varin RA. Application of controlled ball milling in materials processing. In: Srivatsan TS, Varin RA, Khor M, editors. Int. symp. on processing and fabrication of advanced materials IX (PFAM IX). Materials Park, OH: ASM International; 2001. p. 263–87.
[22] Varin RA, Zbroniec L. Decomposition behavior of unmilled and ball milled lithium alanate ($LiAlH_4$) including long-term storage and moisture effects. J Alloys Compd 2010;504: 89–101.
[23] Varin RA, Parviz R. Hydrogen generation from the ball milled composites of sodium and lithium borohydride ($NaBH_4$/$LiBH_4$) and magnesium hydroxide ($Mg(OH)_2$) without and with the nanometric nickel (Ni) additive. Int J Hydrogen Energy 2012;37:1584–93.
[24] Varin RA, Parviz R. The effects of the micrometric and nanometric iron (Fe) additives on the mechanical and thermal dehydrogenation of lithium alanate ($LiAlH_4$), its self-discharge at low temperatures and rehydrogenation. Int J Hydrogen Energy 2012;37:9088–102.
[25] Varin RA, Zbroniec L. Mechanical and thermal dehydrogenation of lithium alanate ($LiAlH_4$) and lithium amide ($LiNH_2$) hydride composites. Crystals 2012;2:159–75.
[26] Varin RA, Zbroniec L, Jang M. Mechano-chemical synthesis of nanostructured hydride composites based on Li–Al–N–Mg for solid state hydrogen storage. Eng Rev 2011;31:111–23.
[27] Van Loon CJJ, De Jong J. Some chlorides with the inverse spinel structure: Li_2TCl_4 (T = Mg, Mn, Fe, Cd). Acta Cryst B 1975;31:2549–50.
[28] Court-Castagnet R, Kaps Ch, Cros C, Hagenmuller P. Ionic conductivity-enhancement of LiCl by homogeneous and heterogeneous dopings. Solid State Ionics 1993;61:327–34.
[29] Robertson AD, West AR, Ritchie AG. Review of crystalline lithium-ion conductors suitable for high temperature battery applications. Solid State Ionics 1997;104:1–11.
[30] Friedrichs O, Buchter F, Borgschulte A, Remhof A, Zwicky CN, Mauron Ph, et al. Direct synthesis of $Li[BH_4]$ and $Li[BD_4]$ from the elements. Acta Mater 2008;56:949–54.
[31] Fichtner M, Fuhr O. Synthesis and structures of magnesium alanate and two solvent adducts. J Alloys Compd 2002;345: 286–96.
[32] Mamatha M, Bogdanović B, Felderhoff M, Pommerin A, Schmidt W, Schüth F, et al. Mechanochemical preparation

and investigation of properties of magnesium, calcium and lithium–magnesium alanates. J Alloys Compd 2006;407:78–86.

[33] Varin RA, Zbroniec L, Polanski M, Bystrzycki J. A review of recent advances on the effects of microstructural refinement and nano-catalytic additives on the hydrogen storage properties of metal and complex hydrides. Energies 2011;4:1–25.

[34] Sandrock G, Gross K, Thomas G, Jensen C, Meeker D, Takara S. Engineering considerations in the use of catalyzed sodium alanates for hydrogen storage. J Alloys Compd 2002;330–332:696–701.

[35] Sandrock G, Gross K, Thomas G. Effect of Ti-catalyst content on the reversible hydrogen storage properties of the sodium alanates. J Alloys Compd 2002;339:299–308.